Finite Element Modeling and Experimental Validation of Interphase Debonding and Particle Fracture in Titanium Carbide/AA1100 Alloy Composites

[1]B. Kotiveera Chari and A. Chennakesava Reddy[2]

[1]Professor, Department of Mechanical Engineering, N.I.T, Warangal, India
[2]Associate Professor, Department of Mechanical Engineering, Vasavi College of Engineering, Hyderabad, India
dr_acreddy@yahoo.com

Abstract: In the current work, the TiC/AA1100 alloy metal matrix composites were subjected to mechanical and thermal loads. The results obtained from the finite element analysis of TiC/AA1100 alloy composites reveal the fracture of TiC particle and separation of interphase from the particle and the matrix. As the volume fraction increases, the particle fracture has been initiated at low temperature of thermal loading.

Keywords: Titanium carbide, AA1100 alloy, RVE model, finite element analysis, interphase debonding, particle fracture.

1. INTRODUCTION

Many properties of metal matrix composites are strongly influenced by the nature of the interphase between reinforcement and matrix. Different coefficients of thermal expansion in the reinforcement and matrix may result in residual stresses in the composite as a result of the fabrication process. Surface energy differences may also give rise to problems through incomplete wetting of the reinforcement by the molten metal, leading to structural weaknesses in the composite and to clumping in the case of particulate reinforced composites. There may also be undesirable chemical reactions between the molten metal and the particle surface, with the possible formation of eutectic compounds. Reactions between the reinforcement and matrix are governed by diffusion, which can be reduced by applying coatings to the particles or by adding alloying elements to the matrix.

The application of surface coatings to the fibers may also help to improve fiber wettability; silica coated carbon fibers are much more readily wet by molten magnesium than uncoated carbon fibers [1]. In mean-field modeling of short-fiber composite materials, a composite unit cell is subjected to mean stress or strain and the effective stiffness or compliance tensors are found by averaging strains and stresses throughout the composite [2-16].

The aim of the present was to assess the effect of thermo-mechanical loading on the fracture in titanium carbide/AA1100 alloy composites was predicted. The shape of titanium carbide nanoparticle considered in this work is spherical. The periodic particle distribution was a square array and corresponding representative volume element (RVE) is showed in figure 1.

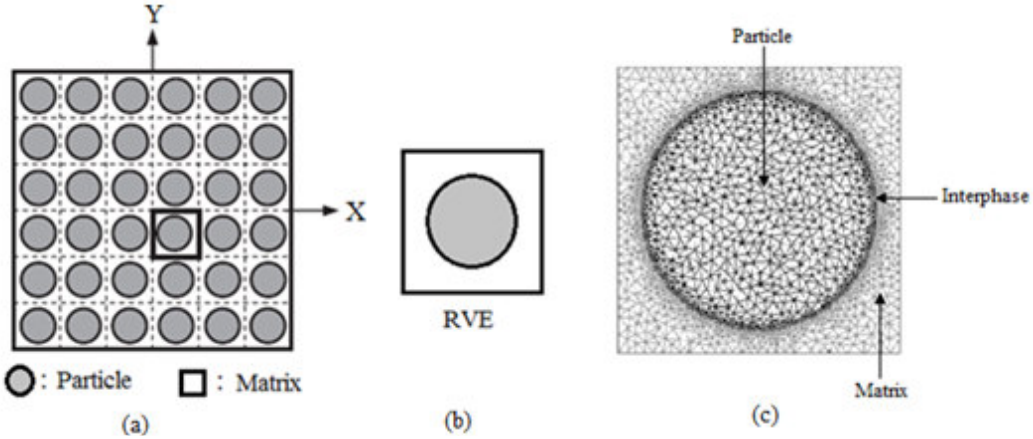

Figure 1: Square array of particles (a); Representative volume element (b); and Discretization of RVE (c).

2. MATERIALS METHODS

The matrix material was AA1100 alloy. The reinforcement material was titanium carbide (TiC) nanoparticles of average size 100nm. The mechanical properties of materials used in the present work are given in table 1.

Table 1: Mechanical properties of AA1100 matrix and TiC nanoparticles

Property	AA1100	TiC
Density, g/cc	2.71	4.93
Elastic modulus, GPa	68.9	400.0
Coefficient of thermal expansion, 10^{-6} 1/^{o}C	21.8	7.4
Specific heat capacity, J/kg/^{o}C	904	565
Thermal conductivity, W/m/^{o}C	220	330
Poisson's ratio	0.33	0.19

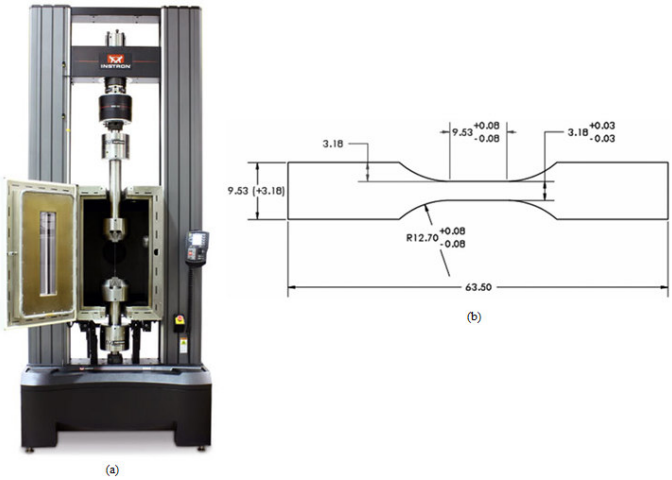

Figure 2: Tensile testing: UTM with temperature controlled chamber and (b) shape and dimensions of tensile specimen.

TiC/AA1100 alloy composites were fabricated by the stir casting process and low pressure casting technique with argon gas at 3.0 bar. The composite samples were give solution treatment and cold rolled to the predefined size of tensile specimens. The heat-treated samples were machined to get flat-rectangular specimens (figure 2) for the tensile tests. The tensile specimens were placed in the grips of a Universal Test Machine (UTM) with temperature controlled chamber at a specified grip separation and pulled until failure. The test speed was 2 mm/min. A strain gauge was used to determine elongation. In the current work, a cubical representative volume element (RVE) was implemented to analyze the tensile behavior TiC/AA1100 alloy composites at two (10% and 30%) volume fractions of TiC and at different temperatures. The large strain PLANE183 element was used in the matrix in all the models. In order to model the adhesion between the matrix and the particle, a CONTACT 172 element was used.

3. RESULTS AND DISCUSSION

The optical micrograph as shown in figure 3 reveals uniform distribution of TiC particles in AA1100 alloy matrix. Agglomeration of TiC particles is also revealed in the microstructures.

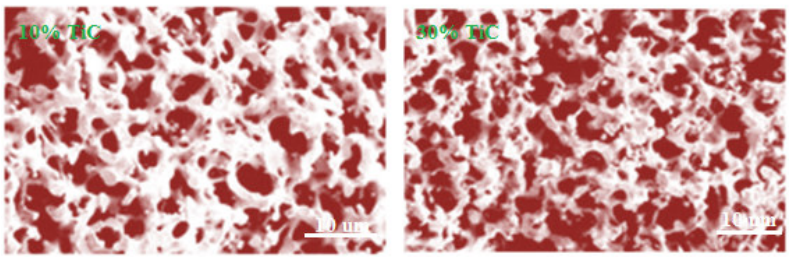

Figure 3: Microstructure showing distribution of TiC nanoparticles in AA1100 alloy matrix.

3.1 Thermo-Mechanical Behavior

Figure 4a shows the normalized elastic modulus of TiC/AA1100 composites at different temperatures. The elastic modulus is normalized with the elastic modulus of AA1100 alloy. When the temperature is increased from 30^{o}C to 300^{o}C, the normalized elastic modulus is decreased. Under thermo-mechanical loading, the stiffness of 30% TiC/AA1100 alloy composites is lower

than that of 10% TiC/AA1100 alloy composites because of the difference in thermal properties of TiC and AA1100 alloy. The normalized stiffness along the normal direction is lower than that along the load direction owing to tensile loading consideration in the present work. The normalized shear modulus and major Poisson's ratio increase with volume fraction of TiC as shown in figures 4b and 4c, respectively. The increase of major Poisson's ratio indicates the elongation along the load is greater than that along the transverse direction of loading of RVE.

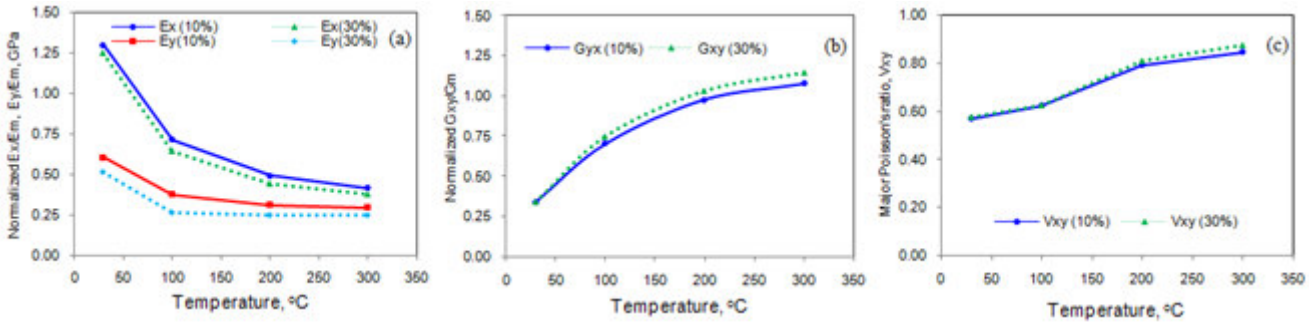

Figure 4: Effect of temperature on micromechanical properties of TiC/AA1100 composites.

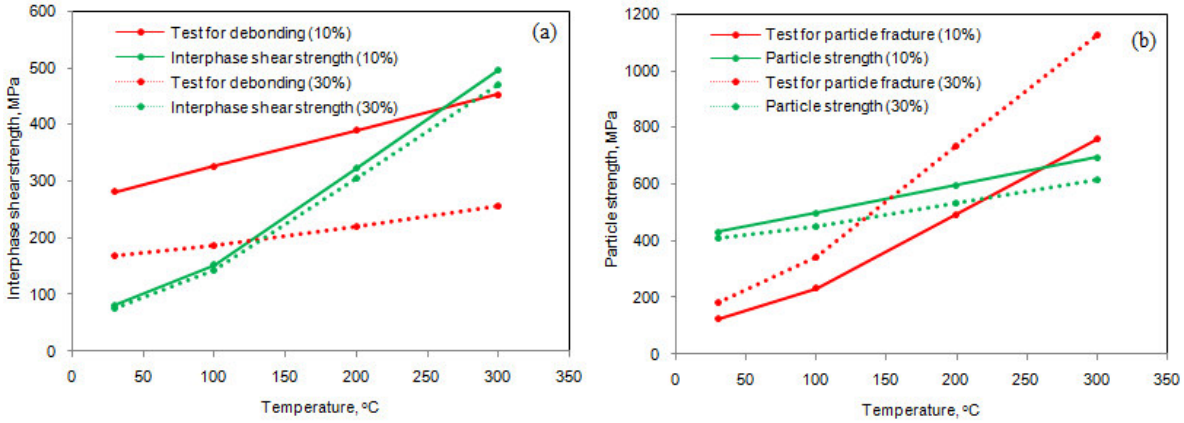

Figure 5: Criterion for interfacial debonding (a) and for particle fracture (b).

3.2 Fracture Behavior

If the particle deforms in an elastic manner (according to Hooke's law) then,

$$\tau = \frac{n}{2}\sigma_p \quad (1)$$

where σ_p is the particle stress. For the interfacial debonding/yielding to occur, the interfacial shear stress reaches its shear strength:

$$\tau = \tau_{max} \quad (2)$$

For particle/matrix interfacial debonding can occur if the following condition is satisfied:

$$\tau_{max} < \frac{n\sigma_p}{2} \quad (3)$$

It is observed from figure 5a that the interphase debonding occurs between TiC nanoparticle and AA1100 alloy matrix as the condition in Eq.(3) is satisfied below 250°C for 10%TiC/AA1100 composites and below 125°C for 10%TiC/AA1100 composites, respectively. The normal displacement field (figure 6) across the interphase increases with increase of temperature. This confirms the increase of interphase separation from TiC particle and AA1100 alloy matrix with increase of temperature. Further, the normal and tangential tractions (figure 7) along the interphase increase with increase of temperature for the cause of interphase separation from TiC particle and AA1100 alloy matrix.

If particle fracture occurs when the stress in the particle reaches its ultimate tensile strength, $\sigma_{p,uts}$, then setting the boundary condition at

$$\sigma_p = \sigma_{p,\,uts} \quad (4)$$

The relationship between the strength of the particle and the interfacial shear stress is such that if

$$\sigma_{P,uts} < \frac{2\tau}{n} \quad (5)$$

Then the particle will fracture. From the figure 5b, it is observed that the TiC nanoparticle was fractured as the condition in Eq. (5) is satisfied above 250°C for 10%TiC/AA1100 composites and above 125°C for 10%TiC/AA1100 composites, respectively. This is due to CTE (coefficient of thermal expansion) and stiffness mismatches between TiC nanoparticles and AA1100 alloy matrix.

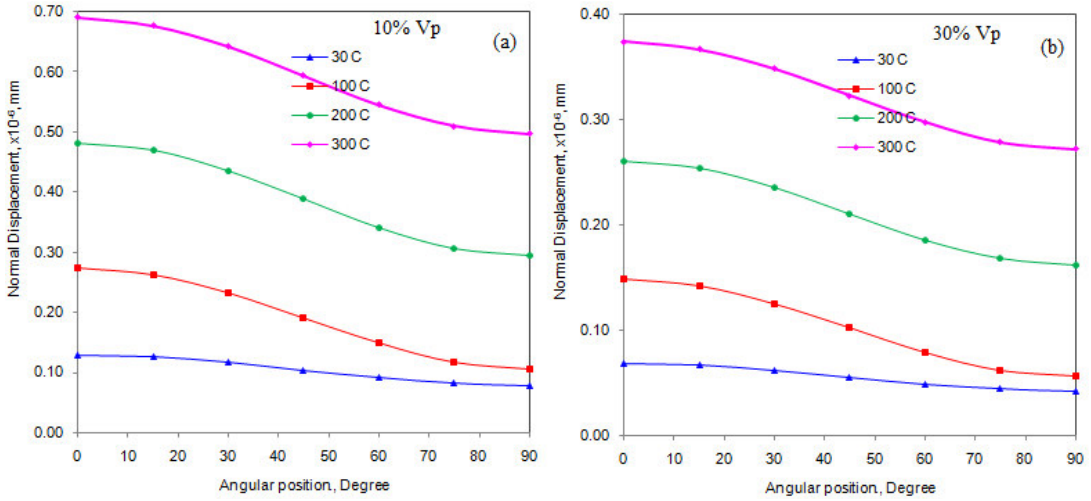

Figure 6: Normal displacement across the interphase between TiC particle and AA1100 alloy matrix.

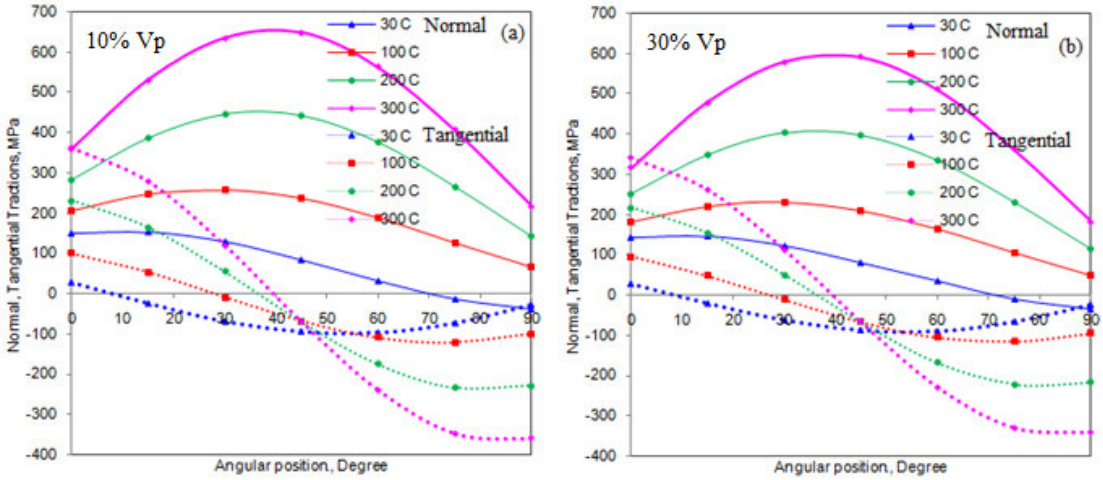

Figure 7: Normal and tangential tractions along the interphase.

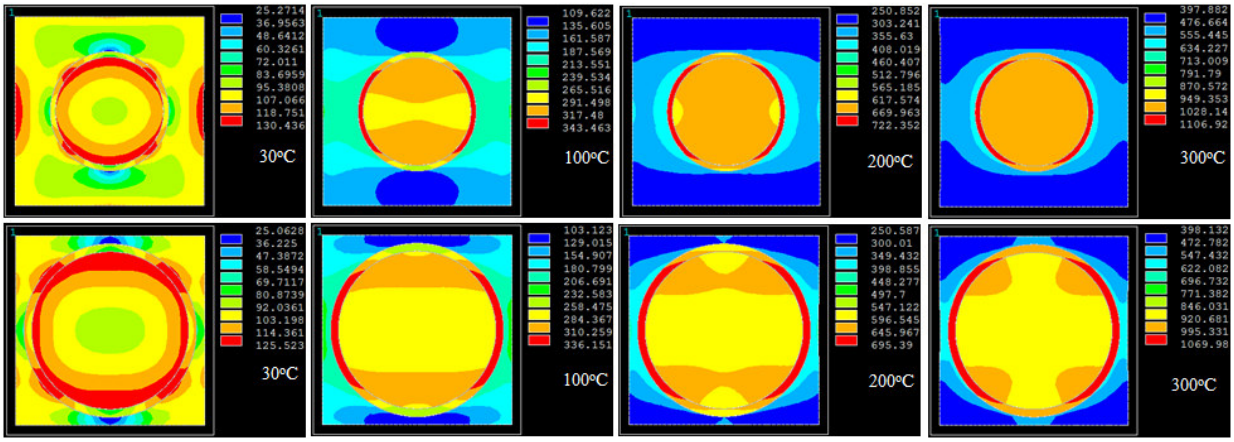

Figure 8: Images of von Mises stresses obtained from FEA: (a) 10%TiC/AA1100 alloy and (b) 30%TiC/AA1100 alloy composites.

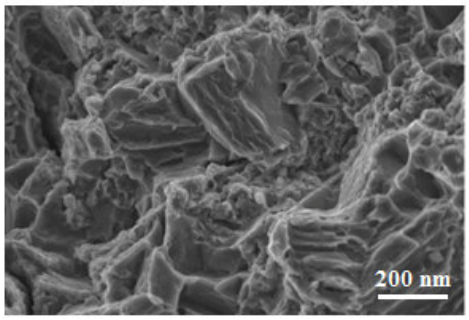

Figure 9: SEM revealing particle fracture in 30%TiC/AA1100 alloy composite.

The von Mises stress as a function of temperature is illustrated in figure 8 from the results obtained from the finite element analysis. The von Mises stresses induced at the interface are higher than that induced in the nanoparticle. Hence, the interphase separation has occurred between the particle and the matrix. The particle fracture was also occurred in TiC/AA1100 alloy composites as the stress induced in the TiC particle exceeds its allowable stress due to thermal shock. The scanning electron micrograph (figure 9) of 30%TiC/AA1100 alloy composite confirms the fracture of TiC particle.

4. CONCLUSION

The microstructure of TiC/AA1100 alloy composites reveals the uniform distribution of TiC nanoparticles in AA1100 alloy. The shear stress is high at the interface resulting to interphase separation from the particle and the matrix. The particle fracture has occurred above 250^{o}C in 10% TiC/AA1100 alloy composites and above 125^{o}C in 30% TiC/AA1100 alloy composites, respectively. The fracture of TiC particle is due to CTE mismatch between TiC and AA1100 alloy.

REFERENCES

1. H. A. Katzman, Fibre coatings for the fabrication of graphite reinforced magnesium composites, Journal of Materials Science, 22, 1987, pp. 144-148.
2. A. Chennakesava Reddy, Evaluation of Debonding and Dislocation Occurrences in Rhombus Silicon Nitride Particulate/AA4015 Alloy Metal Matrix Composites, 1st National Conference on Modern Materials and Manufacturing, Pune, India, 19-20 December 1997, pp. 278-282.
3. A. Chennakesava Reddy, Interfacial Debonding Analysis in Terms of Interfacial Tractions for Titanium Boride/AA3003 Alloy Metal Matrix Composites, 1st National Conference on Modern Materials and Manufacturing , Pune, 19-20 December, 1997.
4. A. Chennakesava Reddy, Assessment of Debonding and Particulate Fracture Occurrences in Circular Silicon Nitride Particulate/AA5050 Alloy Metal Matrix Composites , National Conference on Materials and Manufacturing Processes, Hyderabad, India, 27-28 February 1998, pp. 104-109.
5. A. Chennakesava Reddy, Local Stress Differential for Particulate Fracture in AA2024/Titanium Carbide Nanoparticulate Metal Matrix Composites, National Conference on Materials and Manufacturing Processes, Hyderabad, India, 27-28 February 1998, pp. 127-131.
6. A. Chennakesava Reddy, Micromechanical Modelling of Interfacial Debonding in AA1100/Graphite Nanoparticulate Reinforced Metal Matrix Composites, 2nd International Conference on Composite Materials and Characterization, Nagpur, India, 9-10 April 1999, pp. 249-253.
7. A. Chennakesava Reddy, Cohesive Zone Finite Element Analysis to Envisage Interface Debonding in AA7020/Titanium Oxide Nanoparticulate Metal Matrix Composites, 2nd International Conference on Composite Materials and Characterization, Nagpur, India, 9-10 April 1999, pp. 204-209.
8. H. B. Niranjan, A. Chennakesava Reddy, Computational Modeling of Interfacial Debonding in Fused Silica/AA7020 Alloy Particle-Reinforced Metal Matrix Composites, 3rd International Conference on Composite Materials and Characterization, Chennai, India, 11-12 May 2001, pp. 222-227.
9. H. B. Niranjan, A. Chennakesava Reddy, Nanoscale Characterization of Interfacial Debonding and Matrix Damage in Titanium Carbide/AA8090 Alloy Particle-Reinforced Metal Matrix Composites, 3rd International Conference on Composite Materials and Characterization, Chennai, India, 11-12 May 2001, pp. 228-233.
10. S. Sundara Rajan, A. Chennakesava Reddy, Assessment of Temperature Induced Fracture in Boron Nitride/AA1100 Alloy Particle-Reinforced Metal Matrix Composites, 3rd International Conference on Composite Materials and Characterization, Chennai, India, 11-12 May 2001, pp. 234-239.
11. S. Sundara Rajan, A. Chennakesava Reddy, Estimation of Fracture in Zirconia/AA2024 Alloy Particle-Reinforced Composites Subjected to Thermo-Mechanical Loading, 3rd International Conference on Composite Materials and Characterization, Chennai, India, 11-12 May 2001, pp. 240-245.
12. P. M. Jebaraj, A. Chennakesava Reddy, Finite Element Predictions for the Thermoelastic Properties and Interphase Fracture of Titanium Nitride /AA3003 Alloy Particle-Reinforced Composites, 3rd International Conference on Composite Materials and Characterization, Chennai, India, 11-12 May 2001, pp. 246-251.

13. P. M. Jebaraj, A. Chennakesava Reddy, Effect of Thermo-Mechanical Loading on Interphase and Particle Fractures of Titanium Oxide /AA4015 Alloy Particle-Reinforced Composites, 3rd International Conference on Composite Materials and Characterization, Chennai, India, 11-12 May 2001, pp. 252-256.
14. A. Chennakesava Reddy, Effect of CTE and Stiffness Mismatches on Interphase and Particle Fractures of Zirconium Carbide /AA5050 Alloy Particle-Reinforced Composites, 3rd International Conference on Composite Materials and Characterization, Chennai, India, 11-12 May 2001, pp. 257-262.
15. A. Chennakesava Reddy, Behavioral Characteristics of Graphite /AA6061 Alloy Particle-Reinforced Metal Matrix Composites, 3rd International Conference on Composite Materials and Characterization, Chennai, India, 11-12 May 2001, pp. 263-269.
16. R. Hill, Elastic Properties of Reinforced Solids: Some Theoretical Principles, Engineering Journal of the Mechanics and Physics of Solids, Pergamon Press Ltd. Great Britain, 11, 1963, pp. 357-372420.